

A STRONG-LENS SURVEY IN AEGIS: THE INFLUENCE OF LARGE SCALE STRUCTURE

LEONIDAS A. MOUSTAKAS¹, PHIL MARSHALL², JEFFREY A. NEWMAN^{3,11}, ALISON L. COIL^{4,12}, MICHAEL C. COOPER⁵, MARC DAVIS⁵, CHRISTOPHER D. FASSNACHT⁶, PURAGRA GUHATHAKURTA⁸, ANDREW HOPKINS⁹, ANTON KOEKEMOER¹⁰, NICHOLAS P. KONIDARIS⁸, JENNIFER M. LOTZ^{11,13}, AND CHRISTOPHER N. A. WILLMER⁴

Submitted to the AEGIS ApJL Special Issue

ABSTRACT

We report on the results of a visual search for galaxy-scale strong gravitational lenses over 650 arcmin² of *HST*/ACS imaging in the Extended Groth Strip (EGS). These deep F606W- and F814W-band observations are in the DEEP2-EGS field. In addition to a previously-known Einstein Cross also found by our search (the “Cross,” HST J141735+52264, with $z_{\text{lens}} = 0.8106$ and a published $z_{\text{source}} = 3.40$), we identify two new strong galaxy-galaxy lenses with multiple extended arcs. The first, HST J141820+52361 (the “Dewdrop”; $z_{\text{lens}} = 0.5798$), lenses two distinct extended sources into two pairs of arcs ($z_{\text{source}} = 0.9818$ by nebular [O II] emission), while the second, HST J141833+52435 (the “Anchor”; $z_{\text{lens}} = 0.4625$), produces a single pair of arcs (source redshift not yet known). Four less convincing arc/counter-arc and two-image lens candidates are also found and presented for completeness. All three definite lenses are fit reasonably well by simple singular isothermal ellipsoid models including external shear, giving χ^2_{ν} values close to unity. Using the three-dimensional line-of-sight (LOS) information on galaxies from the DEEP2 data, we calculate the convergence and shear contributions κ_{los} and γ_{los} to each lens, assuming singular isothermal sphere halos truncated at $200 h^{-1}$ kpc. These are compared against a robust measure of local environment, δ_3 , a normalized density that uses the distance to the third nearest neighbor. We find that even strong lenses in demonstrably underdense local environments may be considerably affected by LOS contributions, which in turn, under the adopted assumptions, may be underestimates of the effect of large scale structure.

Subject headings: gravitational lensing – galaxies: high-redshift – large-scale structure of universe – galaxies: individual (HST J141735+52264) – galaxies: individual (HST J141820+52361) – galaxies: individual (HST J141833+52435)

1. INTRODUCTION

Galaxy-scale gravitational lenses have many astrophysical and cosmological applications. These rely on the ability to construct robust and accurate gravitational lens models. However, the contribution of the large-scale structure along the line of sight (LOS) between the observer and the source is often unknown, though it may be significant. In particular, though lens models may detect the influence of the distorting effects of environmental shear (γ) in a preferred direction, models of even the most richly-constrained Einstein Rings with *Hubble Space Telescope* images (e.g. Dye & Warren 2005; Wayth et al. 2005; Koopmans et al. 2006) are

still subject to the mass-sheet degeneracy due to extra field convergence (κ), which can lead to incorrect lens masses (e.g. Kochanek 2004). Indeed, lens galaxies are often massive early-type galaxies, which are generally found in groups or clusters. The most famous example is the two-image lensed QSO Q0957+561 (Walsh et al. 1979; Young et al. 1980). The determination of H_0 from this system depends crucially on correctly modeling the galaxy cluster surrounding the primary lensing galaxy (e.g. Keeton et al. 2000). Several other lens-galaxy groups and environments have been studied in detail (Kundic et al. 1997a,b; Tonry 1998; Tonry & Kochanek 1999; Fassnacht & Lubin 2002; Morgan et al. 2005; Williams et al. 2005; Momcheva et al. 2006; Fassnacht et al. 2006a; Auger et al. 2006), with sometimes inconclusive results. In analyses such as in Keeton & Zabludoff (2004), through mock lens realizations, it is shown how local environment may affect key applications of lenses. They argue that H_0 and Ω_{Λ} may be overestimated, the expected ratio of four-image to two-image lenses may be underestimated, and predictions for millilensing by dark matter substructure may be off by significant amounts. Other theoretical work (Bar-Kana 1996; Metcalf 2005; Wambsganss et al. 2005) suggests that *all* matter along a line of sight can be important.

In the emergent era of large-solid angle, densely-sampled spectroscopic surveys that may include strong lenses, both environmental and large scale structure effects can be explored quantitatively. The DEIMOS spectroscopy of the Extended Groth Strip (EGS) is particu-

¹ JPL/Caltech, 4800 Oak Grove Dr, MS 169-327, Pasadena, CA 91109 leonidas@jpl.nasa.gov

² KIPAC, P.O. Box 20450, MS29, Stanford, CA 94309 pjmc@slac.stanford.edu

³ INPA, LBNL, Berkeley, CA 94720janewman@lbl.gov

⁴ S.O., University of Arizona, Tucson, AZ 85721 acoil, cnaw@as.arizona.edu

⁵ Department of Astronomy, U.C. Berkeley, Berkeley, CA 94720 cooper, marc@astron.berkeley.edu

⁶ Department of Physics, U.C. Davis, Davis, CA 95616 fassnacht@physics.ucdavis.edu

⁸ U.C.O./Lick Observatory, UCSC, Santa Cruz, CA 95064 raja, npk@ucolick.org

⁹ School of Physics, University of Sydney NSW, Australia ahopkins@anu.phyast.pitt.edu

¹⁰ Space Telescope Science Institute, Baltimore, MD 21218 koekemoer@stsci.edu

¹¹ NOAO, 950 North Cherry Street, Tucson, AZ 85719 lotz@noao.edu

¹² Hubble Fellow

¹³ Goldberg Fellow

larly well-suited to this task, and is employed here to both discover new strong galaxy-lenses, and to begin addressing the quantitative effect of environment in their behavior.

The DEEP2-EGS field is a 120×30 arcmin strip, the focus of the ‘‘All-wavelength EGS International Survey’’ (AEGIS), includes deep CFHT *BRI* imaging (Coil et al. 2004a) and Keck/DEIMOS spectroscopy of nearly 14 000 galaxies to date. The spectroscopy is $\sim 75\%$ complete to $R_{AB} < 24.1$. For the analysis here, we only employ the most certain redshift assignments (Coil et al. 2004b). Deep *HST*/ACS imaging of nearly 650 arcmin^2 over 63 stitched tiles reach $V_{606} = 28.75$ and $I_{814} = 28.10$ (AB, 5σ point source; Davis et al, this issue). These data lend themselves to two different techniques for searching for heretofore-unknown gravitational lenses: spectroscopically and visually. The spectroscopic redshifts are supplemented as necessary with photometric redshifts measured from deep KPNO *UBVRI* imaging (A. Hopkins et al., in prep).

The spectroscopic approach of searching for ‘‘anomalous’’ emission lines in early-type spectra has some history (e.g. Warren et al. 1996), and has recently proved to be spectacularly successful when applied to SDSS spectroscopy (Bolton et al. 2004; Willis et al. 2005) with *HST*/ACS followup (Bolton et al. 2005, 2006; Treu et al. 2006). Explicitly spectroscopic searches for lenses in the DEEP2 data will be explored elsewhere.

In the imaging domain, one may hope to search for lens candidates by some automated algorithm, or by visual inspection (e.g. Ratnatunga et al. 1995; Zepf et al. 1997; Fassnacht et al. 2004). The more quantitative and objective automated approach may eventually be preferred (especially for datasets larger than the one considered here), but would, however, require a training set. The EGS ACS data described here is used for just this purpose in a separate work (Marshall et al. in prep) as a precursor to searching the entire *HST* imaging dataset.¹³ Towards that goal we have undertaken a search for lenses by purely visual inspection.

The lens-search methodology is described in §2. The newly discovered lenses and the modeling results are given in §3, while measurements of the local and LOS environments of the lenses are given in §4. Discussion and conclusions are the subject of §5. A concordance flat cosmology with $\Omega_{\Lambda} = 1 - \Omega_m = 0.7$ and $H_0 = 100 h \text{ km s}^{-1} \text{ Mpc}^{-1}$ with $h = 0.7$ is used throughout. Unless otherwise stated, all magnitudes are in the AB system.

2. LENS-SEARCH METHODOLOGY

The search for gravitational lens candidates was conducted by-eye. Three-color images of all of the ACS tiles were built following the Lupton et al. (2004) algorithm, using the photometric zeropoints to provide the relative scale factors, and using the mean of the F606W and F814W images for the green channel. The full ACS dataset was inspected repeatedly in the color images at full resolution, with plausible candidates classified with grades of ‘‘A’’ or ‘‘B’’ and marked for further inspection. Object coordinates were then matched against the DEEP2 spectroscopic catalog, which includes

a ‘‘serendipitous feature’’ flag, for possible anomalous, higher-redshift emission lines. Emission from a source behind the Dewdrop lens (described below) was found in this way.

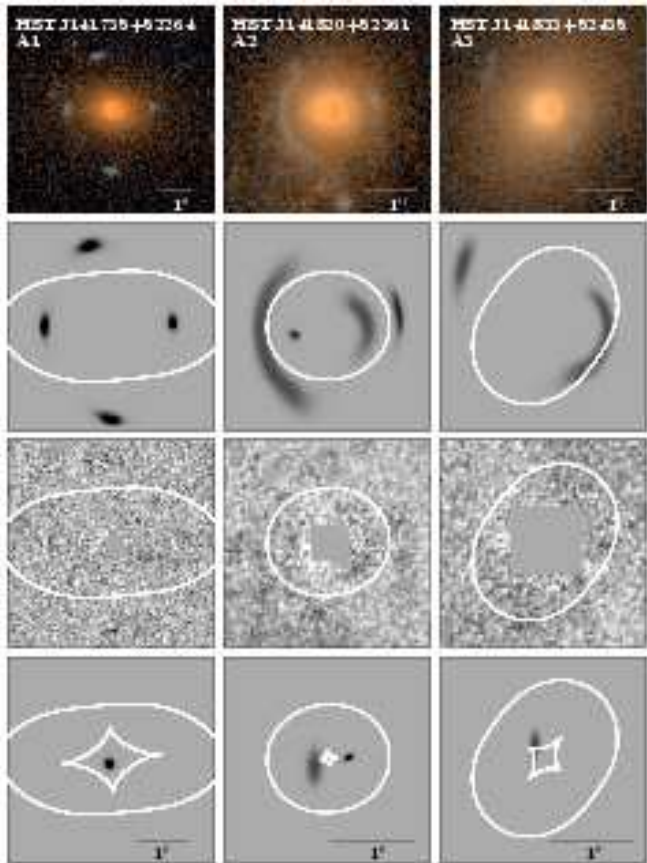


FIG. 1.— The three most plausible lenses from this survey, from left to right the Cross, the Dewdrop, and the Anchor (see text). From top to bottom, we show the discovery image, the lensed image model, the residuals by subtraction with the (lens-galaxy-removed) imaging data, and the reconstructed source. All panels, including the source-plane one, are approximately 3 arcsec on a side, with the exact dimensions shown by the scale bars. The image-plane critical curves and the source-plane caustics are shown in the third and fourth rows, respectively.



FIG. 2.— Additional lens candidates based on visual inspection. These are not yet bolstered by spectroscopy, but will be targeted when possible. The left two are candidate arc/counter-arc lenses, whereas the right two are candidate two-image lenses. Images are 3 arcsec square.

3. LENSES & MODELS

In addition to a previously known Einstein Cross, we find two new unambiguous strong galaxy-galaxy lenses (Fig. 1). Four additional plausible lens candidates (Fig. 2) are also reported on. Here we describe the lens modeling and the model results for each lens.

3.1. Lens modeling and source reconstruction

The lensed sources in the EGS all appear to be blue and extended, and are likely star forming galaxies at high

¹³ <http://www.slac.stanford.edu/~pjm/HAGGLEs>

redshift ($z \sim 1$). We therefore take the image pixels as our data (rather than simply image-centroid positions), and predict the image using a simple ray tracing forward from the source plane, followed by a PSF convolution. We first subtract the lens galaxy light using a tilted 2D Moffat profile,¹⁴ and mask the very center of the lens galaxy where some residual flux remains. It is important that the unmasked region contain not only the lensed images but also the clean pixels that do *not* have lensed features. These clean pixels contain at least as much information as the ones with lensed flux, vetoing models that predict images where there are none. For the projected mass profile of the lens we adopt a singular isothermal ellipsoid (SIE; Kormann et al. 1994) model, plus an external shear component. Using a Markov chain Monte Carlo procedure presented in detail elsewhere (Marshall et al. in prep), the position, ellipticity, orientation and mass of the lens, external shear amplitude and the direction, position, ellipticity, orientation and Sersic profile parameters of the source are all fit to the data. Since we are interested in accurate estimation of the lens environment, we apply a prior on the orientation of the lens ellipticity to reflect the expected correlation with the lens light (e.g. Koopmans et al. 2006).

3.2. *HST J141735+52264 (A1 - Cross)*

This lens was originally discovered by Ratnatunga et al. (1995) by visual inspection of the *HST*/WFPC2 Medium Deep Survey (MDS) data. The lens redshift is $z_{\text{lens}} = 0.8106$ (Table 1), and the source is at $z_{\text{source}} = 3.4$ (Crampton et al. 1996). The large Einstein radius $\theta_E = 1.447$ arcsec and the four-image configuration require a large enclosed mass and a significant amount of external shear, $\gamma_{\text{mod}} = 0.080$, a result consistent with Treu & Koopmans (2004). The best-fit model shows very small residuals at the two outer images, a feature corrected for by Treu & Koopmans (2004) with a potential gradient that is presumably associated with a nearby structure. The mass and external shear are not affected by this correction.

3.3. *HST J141820+52361 (A2 - Dewdrop)*

The Dewdrop lens at $z_{\text{lens}} = 0.5798$ lenses two distinct sources into two pairs of arcs. The Keck/DEIMOS spectrum of the system reveals anomalous [O II] nebular emission at $z_{\text{source}} = 0.9818$ (Fig. 3). The sources in the Dewdrop system are part of a remarkable irregular and loose association of star formation knots and diffuse emitting material that extends over more than 10 arcsec, or more than 80 kpc comoving in size.

3.4. *HST J141833+52435 (A3 - Anchor)*

The Anchor system exhibits a pair of arcs created by a lens at a redshift of $z_{\text{lens}} = 0.4625$. The best-fitting lens model requires a significant external shear contribution (see Table 1), as might be expected from the position and shape of the counter-image to the main arc.

¹⁴ The Moffat function is a modified Lorentzian with variable power law index. The fit is done with the MPFIT IDL suite of C. Markwardt.

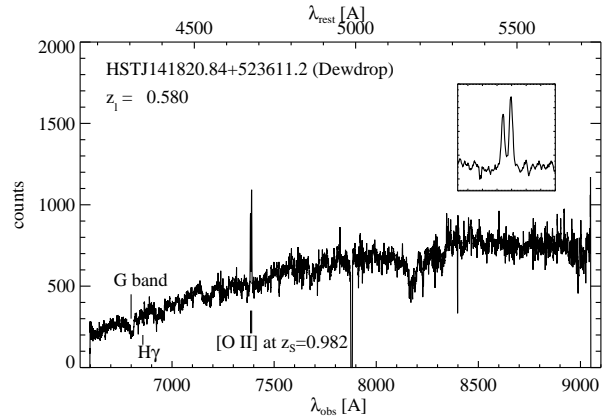


FIG. 3.— The DEIMOS spectrum of the Dewdrop lens clearly shows an “anomalous” doublet emission line (insert), which is readily identified as [O II] at $z_{\text{source}} = 0.9818$.

3.5. *Additional lens candidates*

In Fig. 2 and Table 1 we identify four additional visually-identified lens candidates. Only two of the four presently have redshifts measured, and require further spectroscopic followup. These are presented for completeness, and do not affect the scope or results of this paper.

4. THE ENVIRONMENTS OF THE LENSES

We explore the environments of the lenses in two different ways. The first makes use of a relatively unbiased measure of the very local environment of any one galaxy, dubbed δ_3 and explored in detail in Cooper et al. (2005a,b). This parameter is derived from the distance to the third-nearest neighbor among the galaxies within 1000 km s^{-1} along the line of sight, and scales as the inverse of the cube of this distance. Thus, more concentrated environments have larger values of δ_3 . The typical uncertainties in individual measures of δ_3 are ~ 0.5 dex. We only compute this measure for galaxies with spectroscopic redshifts.

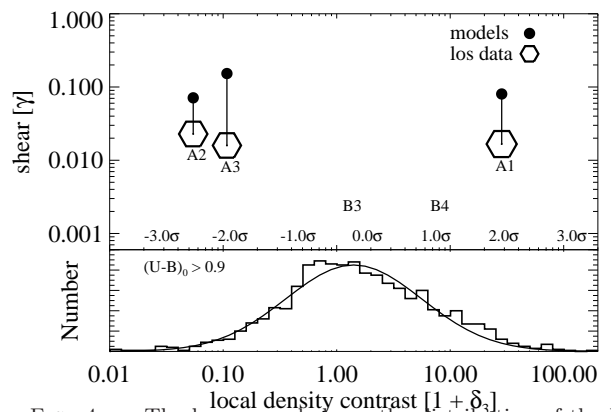


FIG. 4.— The lower panel shows the distribution of the local environmental measure $1 + \delta_3$ (Cooper et al. 2005a), for “red sequence” galaxies with rest-frame colors $(U - B)_0 > 0.9$. (All lenses are found to satisfy the same color-criterion). Based on a gaussian fit to the distribution, $N\sigma$ positions are marked in the x-axis line above, as a guide. The upper panel shows the lens-model and line-of-sight shear for each object, as the filled-circles and open hexagons, respectively. The size of the hexagons corresponds to the calculated line of sight convergence κ_{los} . The $1 + \delta_3$ values of the lens-candidates B3 and B4 are shown as well.

TABLE 1
EGS LENSES: DATA, ENVIRONMENT, & MODELS

		Data						Environment					Models				
ID	Alias	RA (J2000)	Dec (J2000)	z_{lens}	R (AB)	M_B^c (AB)	z_{source}	$\log(1 + \delta_3)$	N_{los}	κ_{los}	γ_{los}	$\theta_{\gamma_{\text{los}}}$ ($^{\circ}\text{E}$)	θ_E ($''$)	σ_{SIS} km s^{-1}	γ_{mod}	$\theta_{\gamma_{\text{mod}}}$ ($^{\circ}\text{E}$)	χ_{ν}^2
A1	Cross	14:17:35.72	52:26:46.3	0.8106	21.38	-21.25	3.40	+1.453	36	0.17	0.02	78	1.45	292.8	0.080	115.3	1.081
A2	Dewdrop	14:18:20.77	52:36:11.3	0.5798	20.55	-20.35	0.9818	-1.260	46	0.10	0.02	140	0.67	260.6	0.071	101.4	1.005
A3	Anchor	14:18:33.11	52:43:52.6	0.4625	20.45	-19.47	...	-0.960	52	0.09	0.02	146	0.83	248.9	0.153	140.8	0.933
B1	Flourish	14:18:07.32	52:30:29.8	0.847 ^a	22.58	(-17.8)
B2	Quotes	14:20:52.01	53:06:57.2	0.601 ^b	23.82	(-16.8)
B3	Dots	14:17:59.01	52:35:14.8	0.6863	21.50	-20.24	...	+0.109
B4	Colon	14:20:53.89	53:06:07.0	0.3545	20.61	-18.47	...	+0.880

a: $\sigma_z = 0.067$ & b: $\sigma_z = 0.24$ (A. Hopkins et al., in prep); c: parenthetical quantities are based on photometric redshifts.

As a second probe of lens environment we model the contribution to the lensing potential due to individual neighboring galaxies using simple analytic mass distributions. We calculate the convergence κ_{los} and shear γ_{los} line-of-sight contribution by all galaxies within a projected separation of $200 h^{-1}$ kpc from the lens galaxies, out to the redshift of the source. We treat each galaxy as an isolated halo, undoubtedly neglecting the effect of group halos and other structures. Assuming that we can approximate each galaxy i as a singular isothermal sphere (SIS), we have $\kappa_i = b_i/2r_i$, where r is the projected distance from the lens and b is the “lens strength” for a background source at angular diameter distances of D_s from the observer and D_{ls} from the lens,

$$b = 4\pi \left(\frac{\sigma_{\text{dm}}}{c} \right)^2 \frac{D_{\text{ls}}}{D_s}. \quad (1)$$

The central dark matter velocity dispersion σ_{dm} of each galaxy is assumed to be the same as the central stellar velocity dispersion, which is derived from the estimated rest-frame B -band (Vega) magnitude of each galaxy using the Faber-Jackson relationship as given in Mitchell et al. (2005) (see also Jönsson et al. 2006). (We neglect the dispersion in this relation). The total shear contribution is the “headless-vector” sum of the shears, $\bar{\gamma}_{\text{los}} = \Sigma \bar{\gamma}_i$, while the total convergence is a scalar sum: $\kappa_{\text{los}} = \Sigma \kappa_i$. It is worth noting that if at large radii the profiles are steeper than SIS (such as NFW), the convergence contribution will be smaller overall than the shear. These measurements are given in Table 1 and discussed in the last section.

5. DISCUSSION & CONCLUSIONS

The numbers of definite lenses reported on here is consistent with other surveys. For example, Bolton et al. (2006) find that $\sim 0.1\%$ of luminous red galaxies are very likely to be strong galaxy-galaxy lenses, although special lines of sight can have much higher lensing rates (e.g. Fassnacht et al. 2006b). The rate above then suggests that there should be ~ 4 strong lenses in this survey, which is a good match to our three.

The main conclusions of this work can be drawn by an examination of Fig. 4. The Cross is in a fairly overdense local environment, which is consistent with this lens being associated with the $z \approx 0.8$ sheet described in Koo et al. (1996) and Im et al. (2002). Given

this, the shear of $\sim 10\%$ required by the model (see also Treu & Koopmans 2004) seems plausible. What seems surprising is that even though both the Dewdrop and Anchor lenses are in *under*-dense environments locally, they still require relatively large shear contributions to produce good fits. In all three cases, we also note the large discrepancy between the modeled and LOS-predicted shear values. To explore this, we ran lens models with external shear and orientation *restricted to the predicted values*, and then examining the resulting models, and particularly the fit χ_{ν}^2 . All three new models require lenses with much higher ellipticity than the light suggests, though in the Dewdrop and the Anchor the formal χ_{ν}^2 remains plausible given the constraints, $\chi_{\nu}^2 = 1.02$ and 1.04 (or underfit by ~ 1 - and ~ 2 - σ), respectively. The new Cross fit, however, is strongly ruled out with $\chi_{\nu}^2 = 2.00$ (or by ~ 75 - σ). This suggests that at least in this case, the inferred LOS influence by SIS dark matter halos is insufficient, and that the large scale structure “sheet” must have an important additional effect.

Our conclusions may be summarized as follows: 1. We have discovered two new strong galaxy-galaxy lenses by visual inspection, with reasonable lens models and source reconstructions. 2. These lenses are drawn from a range of local-density environments, which do not necessarily reflect the influence of unassociated large scale structure. 3. In at least the case of the Cross, the known large scale structure sheet at the redshift of the lens, which is not formally accounted for in the LOS calculation, has a demonstrable effect on the lens model.

We thank Maruša Bradač for discussions. LAM thanks Russell Mirabelli for expert assistance with a GIMP script facilitating the inspection of the ACS data, and UC Berkeley and UC Santa Cruz for their frequent hospitality during the course of this work. The work of LAM was carried out at Jet Propulsion Laboratory, California Institute of Technology, under a contract with NASA. The work of PJM was supported in part by the U.S. Department of Energy under contract number DE-AC02-76SF00515. JAN and ALC are supported by NASA through the *Hubble* Fellowship grants HF-011065.01-A and HF-01182.01-A, respectively.

REFERENCES

Auger, M. W., Fassnacht, C. D., Abrahamse, A. L., Lubin, L. M., & Squires, G. K. 2006, astro-ph/0603448

Bar-Kana, R. 1996, ApJ, 468, 17

- Bolton, A. S., Burles, S., Koopmans, L. V. E., Treu, T., & Moustakas, L. A. 2005, *ApJL*, 624, 21
- . 2006, *ApJ*, 0, 0
- Bolton, A. S., Burles, S., Schlegel, D. J., Eisenstein, D. J., & Brinkmann, J. 2004, *AJ*, 127, 1860
- Coil, A. L., Newman, J. A., Kaiser, N., Davis, M., Ma, C.-P., Kocevski, D. D., & Koo, D. C. 2004a, *ApJ*, 617, 765
- Coil, A. L., et al. 2004b, *ApJ*, 609, 525
- Cooper, M. C., Newman, J. A., Madgwick, D. S., Gerke, B. F., Yan, R., & Davis, M. 2005a, *ApJ*, 634, 833
- Cooper, M. C., et al. 2005b, *ArXiv Astrophysics e-prints*
- Crampton, D., Le Fevre, O., Hammer, F., & Lilly, S. J. 1996, *A&A*, 307, L53
- Dye, S., & Warren, S. J. 2005, *ApJ*, 623, 31
- Fassnacht, C. D., Gal, R. R., Lubin, L. M., McKean, J. P., Squires, G. K., & Readhead, A. C. S. 2006a, *ApJ*, 642, 30
- Fassnacht, C. D., & Lubin, L. M. 2002, *AJ*, 123, 627
- Fassnacht, C. D., Moustakas, L. A., Casertano, S., Ferguson, H. C., Lucas, R. A., & Park, Y. 2004, *ApJL*, 600, L155
- Fassnacht, C. D., et al. 2006b, *ArXiv Astrophysics e-prints*
- Im, M., et al. 2002, *ApJ*, 571, 136
- Jönsson, J., Dahlén, T., Goobar, A., Gunnarsson, C., Mörtzell, E., & Lee, K. 2006, *ApJ*, 639, 991
- Keeton, C. R., Falco, E. E., Impey, C. D., Kochanek, C. S., Lehár, J., McLeod, B. A., Rix, H.-W., Muñoz, J. A., & Peng, C. Y. 2000, *ApJ*, 542, 74
- Keeton, C. R., & Zabludoff, A. I. 2004, *ApJ*, 612, 660
- Kochanek, C. S. 2004, *astro-ph/0407232*
- Koo, D. C., et al. 1996, *ApJ*, 469, 535
- Koopmans, L. V. E., Treu, T., Bolton, A. S., Burles, S., & Moustakas, L. A. 2006, *ApJ*, 0, 0
- Kormann, R., Schneider, P., & Bartelmann, M. 1994, *A&A*, 284, 285
- Kundic, T., Cohen, J. G., Blandford, R. D., & Lubin, L. M. 1997a, *AJ*, 114, 507
- Kundic, T., Hogg, D. W., Blandford, R. D., Cohen, J. G., Lubin, L. M., & Larkin, J. E. 1997b, *AJ*, 114, 2276
- Lupton, R., Blanton, M. R., Fekete, G., Hogg, D. W., O'Mullane, W., Szalay, A., & Wherry, N. 2004, *PASP*, 116, 133
- Metcalf, R. B. 2005, *ApJ*, 629, 673
- Mitchell, J. L., Keeton, C. R., Frieman, J. A., & Sheth, R. K. 2005, *ApJ*, 622, 81
- Momcheva, I., Williams, K., Keeton, C., & Zabludoff, A. 2006, *ApJ*, 641, 169
- Morgan, N. D., Kochanek, C. S., Pevunova, O., & Schechter, P. L. 2005, *AJ*, 129, 2531
- Ratnatunga, K. U., Ostrander, E. J., Griffiths, R. E., & Im, M. 1995, *ApJL*, 453, 5
- Tonry, J. L. 1998, *AJ*, 115, 1
- Tonry, J. L., & Kochanek, C. S. 1999, *AJ*, 117, 2034
- Treu, T., Koopmans, L. V., Bolton, A. S., Burles, S., & Moustakas, L. A. 2006, *ApJ*, 640, 662
- Treu, T., & Koopmans, L. V. E. 2004, *ApJ*, 611, 739
- Walsh, D., Carswell, R. F., & Weymann, R. J. 1979, *Nature*, 279, 381
- Wambsganss, J., Bode, P., & Ostriker, J. P. 2005, *ApJL*, 635, L1
- Warren, S. J., Hewett, P. C., Lewis, G. F., Moller, P., Iovino, A., & Shaver, P. A. 1996, *MNRAS*, 278, 139
- Wayth, R. B., Warren, S. J., Lewis, G. F., & Hewett, P. C. 2005, *MNRAS*, 360, 1333
- Williams, K. A., Momcheva, I., Keeton, C. R., Zabludoff, A. I., & Lehár, J. 2005, *astro-ph/0511593*
- Willis, J. P., Hewett, P. C., & Warren, S. J. 2005, *MNRAS*, 363, 1369
- Young, P., Gunn, J. E., Oke, J. B., Westphal, J. A., & Kristian, J. 1980, *ApJ*, 241, 507
- Zepf, S. E., Moustakas, L. A., & Davis, M. 1997, *ApJL*, 474, L1